2010

Control coordination of a wind turbine generator and a battery storage unit in a remote area power supply system

Nishad Mendis
University of Wollongong, nnrm786@uowmail.edu.au

Kashem Muttaqi
University of Wollongong, kashem@uow.edu.au

Saad Sayeef
saad@uow.edu.au

Sarath Perera
University of Wollongong, sarath@uow.edu.au

Publication Details

N. Mendis, K. M. Muttaqi, S. Sayeef & S. Perera, "Control coordination of a wind turbine generator and a battery storage unit in a remote area power supply system," in 2010 IEEE Power And Energy Society General Meeting, 2010, pp. 1-7.

Control coordination of a wind turbine generator and a battery storage unit in a remote area power supply system

Abstract

A novel hybrid Remote Area Power Supply (RAPS) system consisting of a Doubly Fed Induction Generator (DFIG) based wind turbine and a battery Energy Storage System (ESS) is investigated in this paper. The proposed RAPS system also consists of a dummy load and its controller. The battery energy storage system is used as a buffer which is connected to the DC link of the DFIG. The dummy load which is connected to the AC side of the system is used to absorb the energy associated with over generation, a situation which cannot be handled through the battery system. Control coordination of the dummy load and battery storage system helps maintain the system instantaneous power balance thus ensuring the regulation of the system frequency. The suitability of the proposed RAPS system is assessed in terms of the bandwidth of voltage regulation capability. Small signal model analysis although simpler to perform, is undertaken with a view to compare some of the corresponding results with those obtained using detailed models. Detailed modular simulation of the system is discussed in relation to the system voltage, frequency, DC link stability of the doubly fed induction generator and power sharing among different system components. The model of the entire system has been developed using SimPowerSystem toolbox in MATLAB.

Disciplines

Physical Sciences and Mathematics

Publication Details

N. Mendis, K. M. Muttaqi, S. Sayeef & S. Perera, "Control coordination of a wind turbine generator and a battery storage unit in a remote area power supply system," in 2010 IEEE Power And Energy Society General Meeting, 2010, pp. 1-7.

Control Coordination of a Wind Turbine Generator and a Battery Storage Unit in a Remote Area Power Supply System

Nishad Mendis, *Student Member, IEEE,*, Kashem M. Muttaqi, *Senior Member, IEEE,*, S. Sayeef *Member, IEEE,* and Sarath Perera, *Member, IEEE*

***Abstract*—A novel hybrid Remote Area Power Supply (RAPS) system consisting of a Doubly Fed Induction Generator (DFIG) based wind turbine and a battery Energy Storage System (ESS) is investigated in this paper. The proposed RAPS system also consists of a dummy load and its controller. The battery energy storage system is used as a buffer which is connected to the DC link of the DFIG. The dummy load which is connected to the AC side of the system is used to absorb the energy associated with over generation, a situation which cannot be handled through the battery system. Control coordination of the dummy load and battery storage system helps maintain the system instantaneous power balance thus ensuring the regulation of the system frequency. The suitability of the proposed RAPS system is assessed in terms of the bandwidth of voltage regulation capability. Small signal model analysis although simpler to perform, is undertaken with a view to compare some of the corresponding results with those obtained using detailed models. Detailed modular simulation of the system is discussed in relation to the system voltage, frequency, DC link stability of the doubly fed induction generator and power sharing among different system components. The model of the entire system has been developed using SimPowerSystem toolbox in MATLAB.**

***Index Terms*—Doubly Fed Induction Generator, Remote Area Power Systems, Dummy load, Battery storage system, Small signal model and Control coordination.**

I. Introduction

WITH the increasing energy demand among remote and regional communities, independent power producers are constantly seeking for cost effective means of generating power. Majority of such communities are currently supplied by diesel based generator systems. However, the high cost (ie. fuel, operating and transportation) associated with diesel based generating schemes and growing environmental pressures make that option less favourable [1]. In this regard, hybrid Remote Area Power Supply (RAPS) systems which consist of one or more renewable energy sources incorporated with conventional generating systems can be considered as an attractive alternative. The lower operating cost and reduced carbon emission are known to be the superior features of such systems compared to conventional diesel based generating systems. In a hybrid power system, the selection of the renewable energy source is extremely site specific. Depending on the availability of the renewable energy sources, a proper combination can be used to form a hybrid power system. However, voltage and frequency control, coordination among different system components, power quality (ie. harmonics, voltage unbalance, and flicker) and capital costs associated with such power systems are still major subjects of interest [2] - [3]. In this paper, the first two issues have been addressed.

Relevant to the work presented in this paper, the existing knowledge on hybrid power systems include a grid connected DFIG with a battery storage system [4], frequency control of isolated power system with induction generator based wind turbine together with a flywheel energy storage system [5] and modular simulation of a hybrid power system consisting of an induction generator based wind turbine [6]. However, the control coordination of a hybrid remote area power system consisting of a DFIG, battery and dummy load has received very little or no research attention.

The RAPS system examined in this paper is shown in Fig. 1. The control coordination strategies among various system components are implemented to regulate the system voltage and frequency. In this system, the wind generator can be identified as an uncontrolled energy source whereas the battery storage system operates as a controlled source or sink depending on the operating condition of the system [7] - [10]. The operation of the dummy load is coordinated with the battery to absorb the excessive power of the system. Among the various wind turbine generator technologies available, Doubly Fed Induction Generators (DFIGs) are widely used for wind power application [11] which offer many advantages over other types of wind turbine generators. Power electronic converter rating limited to about 20-30% of the total capacity of the system, maximum power extraction capability in variable wind conditions and ability to generate power in sub-synchronous and super-synchronous modes are the most attractive features of a DFIG system [2]. Although MPPT in the present context (ie. in RAPS systems) is achievable, it is given no emphasis as voltage and frequency control are of greater significance.

In addition to the detailed modular simulation, a small signal stability analysis of the proposed RAPS system has been conducted. In this regard, simplified models (ie. fist order transfer functions) have been used to analyse the power sharing of each system component to regulate the system frequency. The detailed model consists of higher order nonlinear models of the system components which exhibit more accurate system dynamics when compared to the small signal models.

Mr. Nishad Mendis, A/Prof. Kashem M. Muttaqi and A/Prof. Sarath perera are with the School of Electrical, Computer and Telecommunications Engineering, University of Wollongong, and are Members of the Integral Energy Power Quality and Reliability Centre, NSW 2522, Australia (email: nnrm786@uow.edu.au).

978-1-4244-6551-4/10/$26.00 ©2010 IEEE

The paper is organised as follows. Section II outlines the small signal model analysis of the proposed RAPS system. Section III discusses the control methodology adopted for the wind turbine generator, battery energy storage and dummy load and its controller. The control coordination strategies adopted to manage the different system components are discussed in Section IV. The simulated results demonstrating the behaviour of the proposed RAPS system (ie. small signal model and detailed model) for variable load and wind conditions are discussed in Section V. Conclusions are given in Section VI.

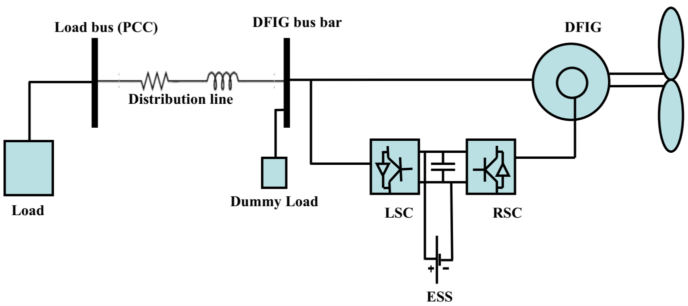

Fig. 1. Proposed Remote Area Power System

II. Small Signal model of the proposed RAPS system

The dynamic analysis of a large power system can be carried out considering its higher order mathematical models incorporating associated nonlinearities. While this is the case, acceptable results can be obtained using simplistic mathematical models for each system component. In this regard, every system component can be modelled as a first order lag transfer function. However, the power losses associated with each system component and its actual controller implementation cannot be explored with this type of an analysis [12] - [13].

In this study, the wind turbine characteristic shown in Fig. 2 is used to emulate the wind turbine. The cut-in wind speed (ie. v_{ci}), rated wind speed (ie. v_r) and cut-out speed (ie. v_{co}) are selected as 7 m/s, 11 m/s and 17 m/s respectively. The turbine power characteristic can be explained using the set of equations given in (4) [14]. The mathematical model of the wind turbine generator and battery system transfer function are given as in (1) and (2) respectively. The time constants of each transfer function are selected by considering the practical operating conditions and characteristics of each component. For example, the time constant of the battery system is very small as it is accompanied by an inverter or converter system depending on its connection interface. Due to the inherent time delay exists between the system frequency variation and the power deviation, the system characteristic equation can be given as in (3). The numerical values of the parameters in each transfer function are listed in TABLE I. A simplified block diagram of the entire RAPS system is shown in Fig. 3. The control strategy discussed in [13] is employed in the current study. The input to the battery controller is taken as the sum of error in supply demand (ie. ΔP_e) and the product of frequency deviation of the system (ie. Δf) and frequency characteristics constant (ie. K_b) of the battery storage system as shown in Fig. 3.

The following assumptions and constraints have been considered in order to simulate a more realistic operating condition for the proposed hybrid RAPS system (ie. for small signal model).

- I : The battery remains connected if its State of Charge (SOC) is within 40%-90%.
- II : The maximum capacity of the battery is only enough to serve 50% of the rated load.
- III : Each system component (ie. wind turbine generator, battery and load) is represented by first order lagging transfer functions neglecting the effect of non-linearities.

$$G_{WTG}(s) = \frac{K_{WTG}}{1+sT_{WTG}} = \frac{\Delta P_{WTG}}{\Delta P_W} \quad (1)$$

$$G_{ESS}(s) = \frac{K_{ESS}}{1+sT_{ESS}} = \frac{\Delta P_{ESS}}{\Delta f} \quad (2)$$

$$G_{SYS}(s) = \frac{\Delta f}{\Delta p_e} = \frac{1}{D+sM} \quad (3)$$

where,
P_W - mechanical power input of a WTG, P_{WTG} - electrical power output of the wind generator, P_{ESS} - energy storage power output, M - equivalent inertia constant and D - damping constant of the system.

$$P_{\mathrm{W}}(t) = \begin{cases} 0 & 0 \le v(t) < v_{ci} \\ (A + Bv(t) + Cv^2(t)) \times P_r & v_{ci} \le v(t) < v_r \\ Pr & v_r \le v(t) < v_{co} \\ 0 & v_{co} \le v(t) \end{cases} \quad (4)$$

where constants A, B, C can be expressed as:

$$A = \frac{v_{ci}}{(v_{ci}-v_r)^2}(v_{ci}+v_r-4v_r(\frac{v_{ci}+v_r}{2v_r})^3) \quad (5)$$

$$B = \frac{v_{ci}+v_r}{(v_{ci}-v_r)^2}(4(\frac{v_{ci}+v_r}{2v_r})^3 - \frac{3v_{ci}-v_r}{v_{ci}+v_r}) \quad (6)$$

$$C = \frac{1}{(v_{ci}-v_r)^2}(2-4(\frac{v_{ci}+v_r}{2v_r})^3) \quad (7)$$

TABLE I
Wind generator, battery storage unit and load transfer function parameters

$K_{WTG} = 1$	$T_{WTG} = 1.5s$	Wind turbine generator
$K_{ESS} = 1$	$T_{ESS} = 0.01s$	Battery storage system
$D = 0.012$	$M = 0.012s$	System load

III. Detailed model of the Proposed RAPS system

With the small signal model in Fig. 3, it is only possible to investigate the frequency regulation capability. However, the precise system dynamics cannot be attained with the simplistic models. Therefore the higher order non linear models should

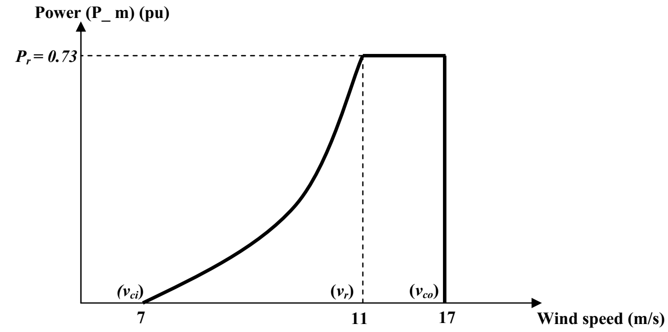

Fig. 2. Power Characteristics of Wind Turbine

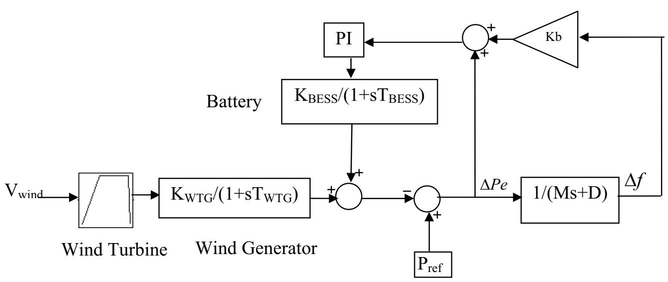

Fig. 3. The Small Signal Block Diagram of the Proposed RAPS System

be employed. In this regard, the detailed modelling and control coordination of the system components are essential to ensure a stable system operation. The following subsections explain the details of modelling aspects of system components and their adopted control strategies individually to each component.

A. Wind Turbine Generator

As the DFIG acts as a major source of energy in the proposed RAPS system, the highest priority/contribution of controlling the system voltage and frequency has to be realised by implementing a robust control scheme on it. In this regard, the vector control strategy described in [15] - [18] can be used as a basis for implementing the DFIG and its associated control. The Rotor Side Converter (RSC) has been used to control the system voltage and frequency whereas the Line Side Converter (LSC) has been used to regulate the DC link voltage regardless of the power flow direction of the back-back converter system. Also it can be designed to provide any additional reactive power to the system when necessary.

Indirect stator flux oriented vector control is adopted in controlling the the RSC. The frequency control of the machine has been realised using (8) - (9). The condition given in (9), is necessary to ensure the indirect stator flux oriented mode of operation of the RSC [18]. With this control, the frequency regulation of the machine is independent of the shaft speed as well as the resistive loading condition of the system. Reactive power control approach has been used to develop the control strategy for voltage control of the machine. It is evident from (10) - (13), that the total stator reactive power consists of two components (ie. Q_{mag} and Q_{gen}). The no load reactive power of the DFIG (ie. Q_{mag}) given by (14) is used for magnetisation purposes. The component which is given by Q_{gen} in (15) is used to provide the reactive power demanded by system loads. With the adopted control strategy, Q_{mag} can be compensated by imposing the condition given by (16). The line side converter control is a conventional arrangement obtained from [18]. Indirect voltage control has been used as the preferred orientation scheme. The complete control diagram of the RSC is shown in Fig. 4.

In addition to the control and provision of excitation requirements discussed above, a method also should exist to provide the excitation current at start. One of the possibilities include self excitation though a capacitor bank connected across the stator terminals as in the case of a self excited asynchronous generator.

$$\phi_{qs} = 0 \tag{8}$$

$$i_{qr} = -\frac{L_s}{L_m} i_{qs} \tag{9}$$

where,
ϕ_{qs} - q component of the stator flux, i_{qr}, i_{qs} - rotor and stator q-axis current respectively, L_s, L_m - stator inductance and magnetising inductance respectively

$$Q_s = -\frac{3}{2} V_{qs} i_{ds} \tag{10}$$

$$Q_s = \frac{3}{2}[-\frac{V_s^2}{\omega L_s} + V_s \frac{L_m}{L_s} i_{dr}] \tag{11}$$

$$i_{dr} = i_{dr\ gen} + i_{mag} \tag{12}$$

$$Q_s = Q_{mag} + Q_{gen} \tag{13}$$

$$Q_{mag} = \frac{3}{2}[-\frac{V_s^2}{\omega L_s} + V_s \frac{L_m}{L_s} i_{dr\ mag}] \tag{14}$$

$$Q_{gen} = \frac{3}{2} V_s \frac{L_m}{L_s} i_{dr\ gen} \tag{15}$$

$$i_{mag} = \frac{V_s}{\omega L_m} \tag{16}$$

where,
V_{qs} - q component of the stator voltage, i_{ds} - stator d-axis current, V_s - stator voltage, i_{mag} - magnetising current, $i_{rd\ gen}$ - fraction of i_{rd} to supply reactive power to the system load and ω - angular frequency at 50 Hz

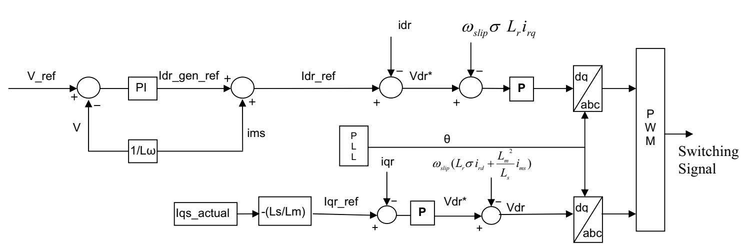

Fig. 4. RSC Control Structure

B. Energy Storage System

In wind based remote power systems, fluctuating power from wind together with varying load profile and relatively low system inertia can result in system instability [19]. Also, demand-generation mismatch in RAPS systems would result in frequency excursions in the system. An energy storage system is one of the best options that can be implemented to overcome such scenarios. Depending upon the system generation and load demand mismatch, an energy storage system could behave either act as a source or a load.

A battery storage system could be identified as a long duration (ie. high energy density) energy storage system compared to other available energy storage options such as super capacitors and flywheel energy storages [7]. In this paper, the battery storage unit is connected to the DC link of the DFIG using a two stage bi-directional DC/DC buck-boost converter. The prime objective of having a battery energy storage system is to minimise the demand generation mismatch as the power balance of the system is important in a remote power system. The adopted control strategy of the battery storage system is shown in Fig. 5. Demand generation mismatch, which is indicated by the term ΔP (ie. difference between wind power and load) in Fig. 5, has been used to generate the reference battery current (ie. $(\mathrm{i_b})_{\mathrm{ref}}$). The $(\mathrm{i_b})_{\mathrm{ref}}$ is compared with the actual battery current (ie. $\mathrm{i_b}$) and the error is compensated through a PI controller. The output of the PI controller is compared with the triangular carrier wave to generate the switching signals (ie. Q_1 and Q_2) for the buck-boost converter.

The estimation of the size of energy storage system is extremely site specific. It is stated in [20] that the ratio given in (17) is an important design parameter that can be used to characterise the capacity of an energy storage needed in a small wind/battery hybrid system. Also it states that this ratio is around 7 in most practical systems. However, in this paper, the sizing of the battery is estimated based on the condition given in (18) - (19). It is assumed that the battery storage system would be able to provide 20% of the system load (ie. 0.2 pu). Also in practical situation, if the converter power ratings considered, the maximum power output of the battery (ie. $(P_{\mathrm{b}})_{\mathrm{max}}$) should be less than the rated power rating of back-to-back converter system (ie. usually it is estimated as 0.3× rated wind power) which can be given by (20). However, in this paper, the converter constraints have not been considered.

$$A = \frac{Battery\ Capacity(Ah)}{Wtg\ Current(A)\ @\ ratedpower} \tag{17}$$

$$(P_{\mathrm{b}})_{\mathrm{max}} = 0.2 \times P_{rated} \tag{18}$$

$$0.2 \times P_{rated} \times (\frac{t}{60}) = (Ah\ rating) \times k \tag{19}$$

$$0.2 \times P_{rated} < 0.3 \times (P_w)_{rated} \tag{20}$$

where,
P_{rated}- rated capacity of the system load, $(P_w)_{rated}$- rated power output of the wind turbine generator, t- time duration that battery provides power into the system and k- average discharge/charge current of the battery in pu

C. Dummy Load and its controller

The dummy load of the system is coordinated with the battery energy storage system to maintain the power balance of the system. In practical RAPS systems a dummy load can be a system which is able to utilise the additional energy, an example of which is a space or water heating system. For simulation studies this could be represented by a set of resistor. However, in this paper, the dummy load consists of a series of resistors which are connected across switches. The resistors operate at zero crossings of the system voltage to ensure minimum impact on the system voltage. The operation of the dummy load is limited only when there is additional power available in the system. The dummy load starts dissipating the additional power after battery bank reaches its rated capacity (ie. $(P_{\mathrm{b}})_{\mathrm{max}}$). The necessary and sufficient condition under which it operates is given by (21). A simplified control scheme of the dummy load controller is shown in Fig. 6.

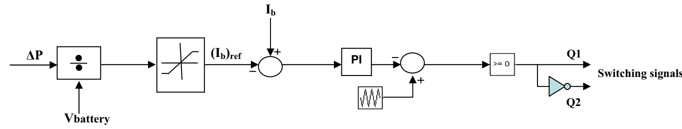

Fig. 5. Battery Control Strategy

$$P_{\mathrm{w}} + (P_{\mathrm{b}})_{\mathrm{max}} - P_{\mathrm{L}} > 0 \tag{21}$$

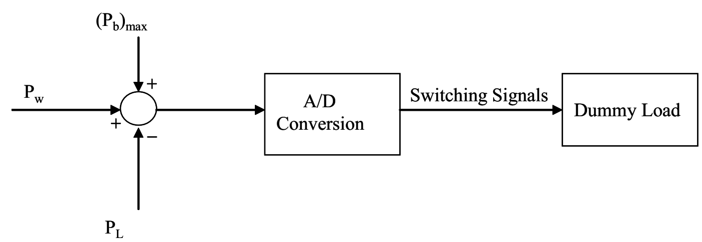

Fig. 6. Dummy Load Control Strategy

IV. CONTROL COORDINATION AMONG DIFFERENT SYSTEM COMPONENTS

As stated earlier, the system voltage and frequency are the most important quantities to be controlled in a RAPS system. At any given moment, the active power balance of the system should be maintained in order to regulate the system frequency. It is stated that if more power flows into the system than the existing load, the system frequency will increase and vice versa. For frequency regulation of the system depicted in Fig.1, the conditions given in (22) - (23) have to be fulfilled. Regulation of the system voltage requires maintaining the reactive power balance of the sources and sinks in the system. This can be expressed using (24) [21].

To maintain the system frequency and achieve acceptable level of voltage regulation at the same time, it is vital to coordinate the active and reactive power balance of the system. A simplified schematic of the control coordination logic associated with the proposed RAPS system is shown in Fig. 7. It shows active power sharing among the different system components to regulate the system frequency. Also, it is assumed that the DFIG is solely responsible for providing total reactive power requirement of the system. Hence, there is no reactive power coordination among the system components. It is entirely handled by the DFIG as discussed in Section III-A.

The details of proposed control coordination strategy depicted in Fig. 7 is as follows. If the power output of the DFIG (ie. P_{w}) is greater than the load power demand (ie. P_{L}) the battery absorbs the additional power (ie. $P_{\mathrm{w}} - P_{\mathrm{L}}$). Otherwise battery enters into its discharge mode of operation. If the excessive generation (ie. P_{w}-P_{L}) is greater than the maximum capacity of the battery (ie. $(P_{\mathrm{b}})_{\max}$) then the dummy load has to consume the additional power associated with the RAPS system. If the dummy power (ie. P_d) is higher than its maximum rating (ie. $(P_{\mathrm{d}})_{\max}$), then the wind turbine pitch regulation has to be activated to control the active power flow of the system. Further, it is assumed that P_{w} and P_{b} are sufficient to supply the system loads at all times.

$$\Sigma P_{sorces} - \Sigma P_{sinks} = \frac{dK.E}{dt} = \frac{d\Sigma J\omega^2}{dt} = 0 \quad (22)$$

$$P_w \pm P_b = P_L + P_d \quad (23)$$

where,
P- active power, K.E- kinetic energy of the system, J- moment of inertia of rotating machine and ω- angular velocity of the rotating machine.

$$\Sigma Q_{sources} - \Sigma Q_{sinks} = 0 \quad (24)$$

where,
Q- reactive power of the system

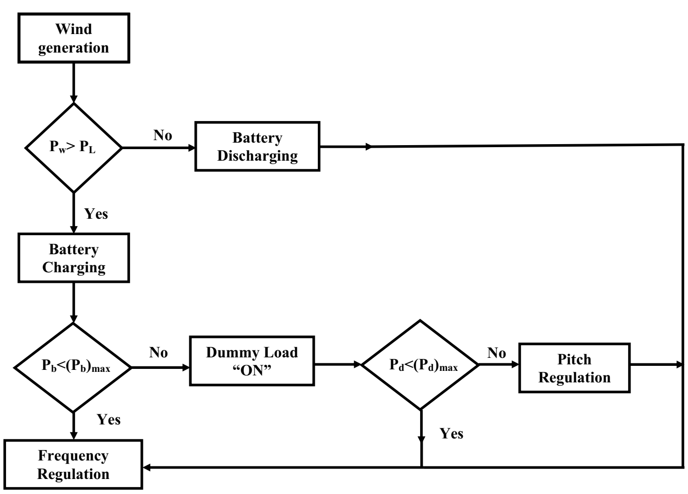

Fig. 7. Control Coordination of Proposed RAPS System

V. Simulation Results

The dynamics of the hybrid power system depicted in Fig. 1 has been studied using its small signal model shown in Fig. 3. In this regard, active power sharing of various components have been observed. As stated previously, modular simulation of the hybrid power system with detailed models is also presented. In this scenario, the coordination of the different system components is the most critical and important aspect to be investigated for stable operation of the entire system.

The response of the proposed RAPS systems using small signal and detailed model are investigated under (a) variable load and (b) variable wind speed.

A. Small Signal Hybrid Model

The simulated behaviour of the hybrid power system is shown in Fig. 8. The wind velocity variation is shown in Fig. 8-(a). The corresponding wind power output is depicted in Fig. 8-(b). When the wind velocity is nearly 12 m/s, the corresponding wind power output from the wind generator is 0.73 pu. From Fig. 8-(e), it can be seen that, the system load is at 0.6 pu. The excess power (ie. $P_{\mathrm{L}} - P_{\mathrm{w}}$), 0.13 pu, is absorbed by the battery bank as evident from Fig. 8-(c). The wind velocity drops to nearly 10 m/s at t = 75 seconds. The corresponding wind power output is about 0.6 pu. The power imbalance (ie. ΔP) is served by battery storage unit. At time t = 150 seconds, the load power increases to 1 pu. It can be seen that the battery storage unit now supplies nearly 0.4 pu power to the system to maintain the system power balance. Also, the battery State of Charge (SOC) is shown in Fig. 8-(d). Initially it is at 80% and remains constant until t = 150 seconds. After t = 150 seconds, the SOC of the battery drops as it discharges power into the system. The power imbalance associated with the system (ie. $P_{\mathrm{w}} \pm P_{\mathrm{b}} - P_{\mathrm{L}}$) shown in Fig. 9-(a). It can be seen that the the power imbalance of the system is always maintained nearly zero. The corresponding system frequency deviation (ie. Δf) is shown in Fig. 9-(b). Upon close examination, it can be seen that the frequency of the system is regulated within $\pm 0.1\%$. As expected, the highest frequency deviation is seen to be occurred at t = 150 seconds during the step load change.

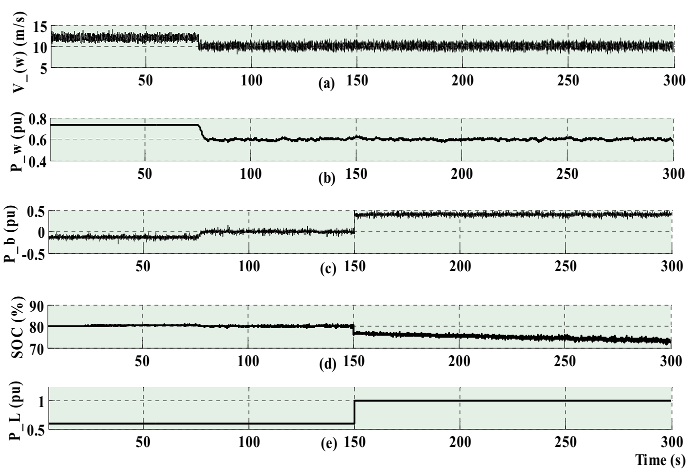

Fig. 8. Power Sharing of the RAPS System at Variable Wind and Load Conditions. (a) Wind Speed, (b) Wind Power, (c) Battery Power, (d) State of Charge of Battery and (e) System Load

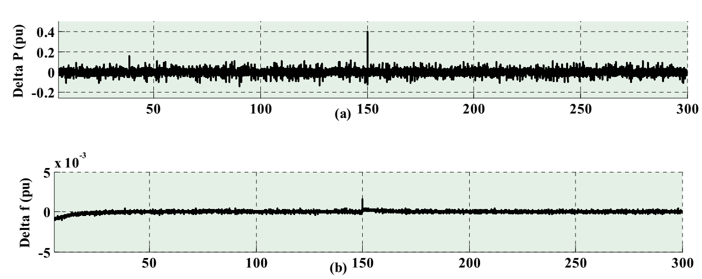

Fig. 9. (a) Power Imbalance and (g) Frequency Deviation of the System

B. Detailed Hybrid model

The entire RAPS system has been simulated under variable wind and load conditions. Fig. 10 shows the system response whereas Fig. 11 shows the power sharing among different system components. In order to compare with the small signal model, similar case of variable wind and load conditions have been used.

The wind condition under which the system has been simulated is shown in Fig. 10-(a). It can be seen that the wind velocity of the system is initially 11 m/s. At t = 2 seconds, the wind velocity of the system has been changed to 9 m/s. Also, the system load consists of 0.3 pu resistive load. At time t = 4 seconds, the load has been increased to a value of 0.6 pu as shown in Fig. 11-(d). The system voltage at PCC is shown in Fig. 10-(b). It can be seen that the voltage is not seen to be affected by the wind speed change but with resistive load step up. At the time of load step up (ie. at t = 4 seconds) the system voltage drops to 0.96 pu but recovers to its rated value soon after. However, the load side voltage of the system stays within $\pm 1\%$ during its normal operation. Fig. 10-(c) shows the system frequency. As expected, it is almost regulated at its rated value of 1 pu. The frequency of the system is not seen to be affected by the wind speed change. However, it can be seen that, with the resistive load step up, the frequency excursion of the system is comparatively high compared to the variable wind scenario. The highest frequency deviation of the system which occurs at t = 4 seconds, seen to be limited to 0.25 Hz. The DC link voltage of the DFIG is depicted in Fig. 10-(d). The simulated behaviour of the DC link shows that it is well regulated at its rated value throughout the operation except during the resistive load step change. During the resistive load step change, the battery storage unit abruptly changes its direction of power (ie. charing to discharging mode of operation) as evident from Fig. 11-(b). This instantaneous power flow reversal causes the DC link voltage fluctuation which can be described by using capacitor voltage equation (ie. ($i_c = C\frac{dV}{dt}$)). At the time of load step up the DC link voltage variation stays within $+10\%$ and -5%.

The wind power variation of the system is shown in Fig. 11-(a). For simulation purposes, initially the slip of wind turbine is set to s = -0.1 which corresponds to super synchronous mode of operation. According to the wind turbine characteristics, the corresponding maximum power output of the wind generator is 0.73 pu at a shaft speed of 1.2 pu for 11 m/s wind speed. From Fig. 11-(a), the power output of the DFIG is seen to rise to a value of 0.625 pu. At this time the load demand set to 0.3 pu. The additional power is shared between the battery storage unit and dummy load. However, the battery storage maximum power capacity is limited to 0.2 pu as shown in Fig. 11-(b). Hence, the remanning power (ie. $P_{\mathrm{w}} - P_{\mathrm{L}} - P_{\mathrm{b}}$) is consumed by the dummy load as evident from Fig. 11-(c). At time t = 2 seconds the wind velocity drops to 9 m/s causing a reduction in the power output of the wind turbine generator. As a result, the dummy load power consumption is also reduced until the load step up change that occurs at time t = 4 seconds. At the instance of resistive load step up, (ie. at t = 4 seconds), the load power exceeds the wind generator power output and the dummy load power is set to zero. At the same time, the battery changes its mode of operation from charging to discharging to maintain the system power balance. The frequency deviation of the system (ie. Δf) and active power imbalance (ie. ΔP) associated with the system is shown in Fig. 12. As expected the highest frequency and active power deviation are seen to occur during the load step up at t = 4 seconds. Thereafter, the power imbalance (ie. $P_{\mathrm{w}} \pm P_{\mathrm{b}} - P_{\mathrm{L}}$) of the system settles down at 0.012 pu whereas the system frequency deviation maintains within ± 0.005 pu showing a similar simulated behaviour with the results that obtained from the small signal model analysis.

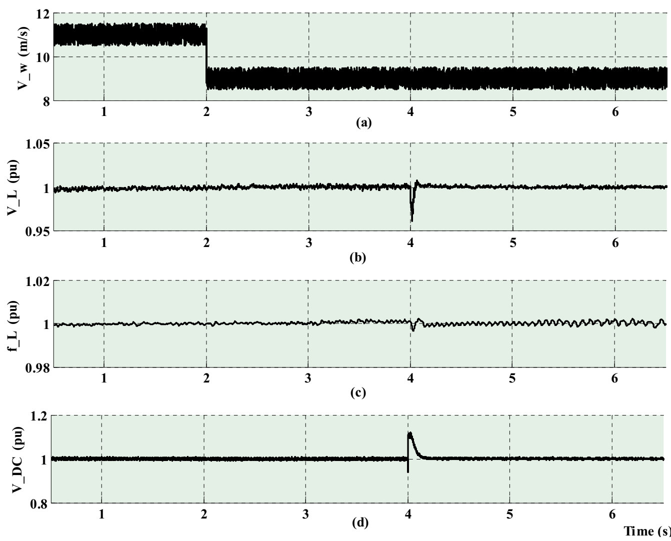

Fig. 10. Response of the RAPS System at Variable Wind and Load Conditions. (a) Wind Speed, (b) Voltage at PCC, (c) Frequency at PCC, and (d) DC link Voltage

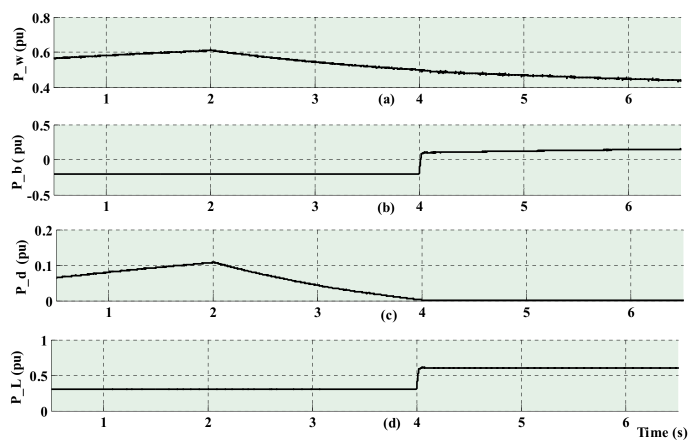

Fig. 11. Power Sharing of the RAPS System at Variable Wind and Load Conditions. (a) Wind Power, (b) Battery Power, (c) Dummy Power and (d) System Load

VI. Conclusions

This paper has investigated the hybrid operation of a novel DFIG based remote area power system. The system performance has been investigated in relation to the bandwidth of the voltage regulation capability under variable load and wind conditions. Frequency regulation is investigated using both small signal and detailed model analysis. Both types of modelling and simulation exhibit comparable results for active

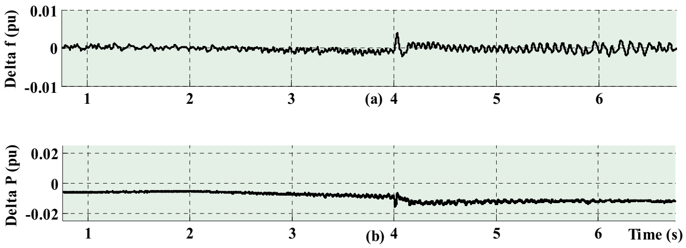

Fig. 12. Frequency and Power Deviation of the System (a) Frequency Deviation and (b) Active Power Imbalance

power sharing and frequency behaviour of the system. It is seen that the proposed RAPS system is capable of regulating both the voltage and frequency within acceptable limits. The proposed control coordination for the detailed model works well as anticipated. Power sharing among the different system components together with their individual controls contribute to maintain the system voltage and frequency within the acceptable limits. However, smooth transition of battery operation mode (ie. charging to discharge and vice versa) is essential to avoid DC link voltage fluctuation of the DFIG.

References

[1] T. Senjyu, T. Nakaji, K. Uezato and T. Funabashi, "A Hybrid Power System Using Alternative Energy Facilities in Isolated Island", *IEEE Transaction on Energy Conversion*, vol. 20, issue 2, Jun 2005, pp. 406 - 414.

[2] N. Mendis, K. Muttaqi and S. Perera, "Voltage quality behaviour of a wind turbine based Remote Area Power System", *International Conference on Industrial Electronics, Gibsland, Australia*, Jun 10-13 Feb. 2009, pp. 1-6.

[3] Technical report AS61400.21, 2006, "Wind Turbines - Measurement and Assessment of Power Quality Characteristics of Grid Connected Wind Turbines".

[4] C. A. Abbey and G. Joos, "Integration of energy storage with a doubly-fed induction machine for wind power applications", *35th Annual IEEE Power Electronics Specialist Conference, Aachen, Germany*, vol. 3, 20-25 Jun. 2004, pp. 1512 - 1521.

[5] R. Takahashi and J. Tamura, "Frequency control of isolated power system with wind farm by using Flywheel Energy Storage System", *18th International conference on Electrical Machines, Vilamoura, Portugal*, 6-9 Sept. 2008.

[6] E.Muljadi and J. T. Bialasiewicz, "Hybrid Power System with Controlled Energy Storage", *29th Annual Conference of IEEE industrial Society, Virginia*, 2-6 Nov. 2003.

[7] L. Wei and G. Joos, "A Power Electronic Interface for a Battery Supercapacitor Hybrid Energy Storage System for Wind Applications", *Power Electronics Specialists Conference, Rhodes, Greece* , 15-19 Jun 2009.

[8] J. Zhenhua and Y. Xunwei, "Modeling and control of an integrated wind power generation and energy storage system", *Power and Energy Society General Meeting 2009, Calgary, Alberta, Canada*, 26-30 July 2009, pp. 1 - 8.

[9] C. A. Abbey and G. Joos, "Short-term energy storage for wind energy applications", *Industry Application conference 2005, Hong Kong* , vol. 3, 2-6 Oct. 2005, pp. 2035 - 2042

[10] A. Boyette, P. Poure and S. Sadate, "Constant Gird Power Control of Wind Turbines with DFIG and Long Duration Storage Unit", *International Journal of Distributed Energy Resources*, vol.3, Sept. 2006, pp.63-82.

[11] S. Li and T.A Haskew ,"Analysis of Decoupled d-q Vector Control in DFIG Back-to-Back PWM Converter", *Power Engineering Society General Meeting, Tampa, Florida*, 24-28 Jun 2007, pp. 1 - 7.

[12] D. J Lee and L. Wang "Small-Signal Stability Analysis of an Autonomous Hybrid Renewable Energy Power Generation/Energy Storage System Part I: Time-Domain Simulations ", *IEEE Transaction on Energy Conversion*, vol 23, 28 Mar. 2008, pp. 311-920.

[13] T. Senjyu, T. Nakaji, K. Uezato, T. Funabashi "A Hybrid Power System Using Alternative Energy Facilities in Isolated Island", *IEEE Transaction on Energy Conversion*, vol. 20, June 2005, pp. 406 - 414.

[14] P. Giorsetto, K. F. Utsurogi, "Development of A New Procedure for Reliability Modeling of Wind Turbine Generators", *IEEE Trans. Power Apparatus and Systems*, vol. PAS-102, Jan 1983 pp. 134 - 143.

[15] D. Forchetti, G. Garcia and M. I. Valla, "Vector control strategy for a doubly-fed stand-alone induction generator", *The 28th Annual Conference of the IEEE Industrial Electronics Society, Sevilla, Spain*, vol. 2, 5-8 Nov. 2002, pp. 991 - 995.

[16] P. Ling, L. Yongdong, C. Jianyun, Y. Guofeng, "Vector Control of a Doubly Fed Induction Generator for Stand-Alone Ship Shaft Generator Systems", *International Conference on Electrical Machines and Systems, Wuhan, China*, 8-11 Oct. 2007, pp. 1033 - 1036.

[17] F. Khatounian, E. Monmasson, F. Berthereau, E. Delaleau and J. P. Louis, "Control of a Doubly Fed Induction Generator for Aircraft Application", *Industrial Electronics Society,IEEE 29th Annual Conference, Roanoke, Virginia, USA*, vol. 3, 2-6 Nov. 2003, pp. 2711 - 2716.

[18] R. Pena, R. Cardenas, G. M. Asher J. C. Clare, J. Rodriguez and P. Cortes, "Vector Control of a Diesel-Driven Doubly Fed Induction Machine for a Stand-Alone Variable Speed Energy System", *Industrial Electronics Society, IEEE 28th Annual Conference, Sevilla, Spain*, vol. 2, 5-8 Nov. 2002, pp. 985 - 990.

[19] Y. Zhou, J. A. Ferreira and P. Bauer, "Grid-connected and islanded operation of a hybrid power system", *PowerAfrica 2007, Johannesburg, South Africa*, 16-20 Jul 2007, pp. 1-6.

[20] D. Corbus, C.Newcomb, E.I Baring-Gould and S. Friedly, "Battery Voltage Stability Effects on Small Wind Turbine Energy Capture", *AWEA WINDPOWER - Portland*, 2-5 June 2002.

[21] S. M. Drouilhelt, "Power Flow Management in a High Penetration Wind-Diesel Hybrid Power System with Short-Term Energy Storage", *Windpower Conference, Burlington, Vermont*, Jun 20-23 1999.

ACKNOWLEDGEMENT

This work is supported by the Australian Research Council (ARC) and Hydro Tasmania Linkage Grant, LP0669245. The authors gratefully acknowledge the support and cooperation of Hydro Tasmania personnel in providing data and advice on the operation of remote area power supply system.

N. Mendis received his B.Sc.(Eng) (Hons.) degree in electrical power engineering from the University of Moratuwa, Sri Lanka. Currently he is pursuing studies towards the Ph.D. degree at the University of Wollongong, Australia. His research interests are renewable energy technologies and electrical machine modelling.

K. M. Muttaqi (M'01, SM'05) received the Ph.D. degree from Multimedia University, Malaysia, in 2001. Currently, he is an Associate Professor at the School of Electrical, Computer, and Telecommunications Engineering, University of Wollongong, Wollongong, Australia. He was associated with the University of Tasmania, Australia as a Research Fellow/Lecturer/Senior Lecturer from 2002 to 2007, and with the Queensland University of Technology, Australia as a Research Fellow from 2000 to 2002. Previously, he also worked for Multimedia University as a Lecturer for three years.

S. Sayeef graduated from the University of Auckland, New Zealand, with a Bachelor of Engineering (First Class Honours) degree in Electrical and Electronic Engineering in 2002. He received the Ph.D. degree in 2009 from the University of New South Wales, Sydney. He joined the School of Electrical, Computer and Telecommunications Engineering at the University of Wollongong in February 2009 as an Associate Research Fellow.

S. Perera (M'95) received the B.Eng. degree in electrical power engineering from the University of Moratuwa, Sri Lanka, the M.Eng. degree from the University of New South Wales, Sydney, Australia, and the Ph.D. degree from the University of Wollongong, Wollongong, Australia. He had been a lecturer at the University of Moratuwa. Currently he is an Associate Professor with the University of Wollongong, where he is also the Technical Director of the Integral Energy Power Quality and Reliability Centre.